SCALING RESISTANCE OF STAINLESS STEELS MADE BY PM

Prasan Samal *(North American Hoganas)*, Owe Mars, Ingrid Hauer, and Barbara Maroli *(Hoganas AB)*

ABSTRACT

In North America, legislative pressures to minimize pollution from motor vehicles are placing greater demands on the vehicle exhaust systems. Because of this, and the increasing market demand for long-term vehicle warranties, conversion to all stainless steel exhaust systems have been progressing steadily since mid-1990s. All stainless steel exhaust systems are expected to become more popular in Europe and Asia as well, in response to similar legislative agenda. In an all stainless steel exhaust system, PM stainless steel exhaust flanges and HEGO bosses are frequently selected over wrought (stamped and formed) stainless steel components. This is because PM stainless steel provides significant advantages in performance, cost and design flexibility, over their wrought counterparts. The improved performance is primarily due to the fact that PM stainless steel is more resistant to spalling of oxide scales in application-specific cyclic oxidation tests, compared to wrought stainless and wrought carbon steels.

This paper investigates the cause of the superior resistance to scaling of PM stainless steels in these oxidation tests. Stainless steel flanges made of 400 series alloys, via PM and wrought processes, were investigated to determine the rate of the oxide scale build up, and the subsequent spalling of the scale. Microstructural examinations revealed major differences in the characteristics of the scale formed in these two types of materials. The lower coefficient of thermal expansion, combined with the beneficial effect of pore-scale interaction, are found to be responsible for stronger adherence of scale to the metal substrate in the case of PM, which in turn prevents spalling of the scale during thermal cycling.

INTRODUCTION

In the mid 1990s the US auto industry began to convert major components of the automobile exhaust system from plain carbon and low alloy steels to wrought and PM stainless steels. This transition was necessitated by two factors: (1) With the increasing market demand for extended vehicle bumper-to-bumper warranties, it became essential to enhance the durability and serviceability of the exhaust system so to be in par with the rest of the vehicle. (2) The Federal

Clean Air Act passed in 1987, imposed restrictions on vehicle emissions covering the life span of the vehicle. Since its passage, however, the target dates for meeting specific emission limits have been extended. Nevertheless, OEMs and Tier 1s continue their efforts to achieve significantly lowered leak rates over the life span of the vehicle. Use of stainless steel also supports the long-term objective of increasing engine operating temperatures, which is essential for enhancing engine performance and fuel efficiency.

Conversion from thick, low carbon steel exhaust flanges to wrought, and PM stainless steel, was preceded by the conversion of exhaust tubing to wrought 409L stainless steel - which in addition to being a low cost stainless steel, offers excellent formability, weldability and adequate resistance to corrosion. Subsequently grades 409L and 434L, processed via both wrought and PM routes, were proven to be optimum materials for the manufacture of exhaust flanges and HEGO bosses. These alloys offer adequate room and elevated temperature mechanical strengths, as well as sufficient resistance to elevated temperature oxidation and wet corrosion. These materials also match the coefficient of thermal expansion of the 409L tubing, thus minimizing thermal fatigue of components in the assembly. In PM, two versions of 409L are currently in use. One of these is the standard PM 409L, which has a chromium content of 10.50 to 11.75%, while the other, designated as 409LE has a chromium content of 11.50 to 13.5%. Both grades contain approximately 0.5% columbium as the stabilizer, whereas, the wrought 409L may contain titanium solely, or titanium plus columbium as the stabilizer. Wrought and PM 409L/409LE are low carbon alloys with a maximum carbon content of 0.03%.

In flange designs that require high strength, but do not involve welding, wrought high carbon martensitic stainless steels, such as wrought 410Cb, are also specified. Wrought alloy 410Cb contains 11.5% chromium, 0.25% columbium and 0.12% carbon. This alloy is heat treatable. The role of columbium here is to form columbium carbide precipitates in a martensitic matrix, which lends to flexibility in the heat treating process and enhances toughness [1].

Primarily, the function of the flange is to form an airtight joint between the connecting components of the exhaust system, as well as to retain the tightness of the joint in the face of significant mechanical and thermal cycling, and periodic exposure to corrosive conditions arising from road de-icing salts. Besides exhibiting adequate mechanical strength and corrosion resistance, the flange material should be moderately resistant to oxidation and thermal fatigue. Dimensional accuracy, flatness and surface finish of the component are also important criteria for ensuring a no leak (or low leak) assembly.

Two application-specific tests are currently in use for qualification of exhaust flanges. Both of these are accelerated tests. The High Temperature Oxidation/Corrosion Test (HTOT) is designed to test the flange material for its resistance to corrosion, elevated temperature oxidation, and thermal fatigue. The Hot Vibration Leak Test (HotVib) is an actual leak rate test which is performed on a "flange-manifold-tubing" assembly while the assembly is being subjected to a specified schedule of thermal and mechanical cycling [2]. The HTOT test is designed to determine the ability of the flange material to withstand the harsh environments which the component would see in actual use. During use, an exhaust flange would reach temperatures in the neighborhood of 600^0C (in air); become covered with road de-icing salts, and when the vehicle would pass over a puddle of water it would be subjected to rapid quenching. The optimum flange material should withstand the combined effects of exposure to elevated temperatures, corrosive environment arising from de-icing salts, and the drastic thermal cycling, without significantly losing its integrity and functionality, over the life span of the vehicle.

In the High Temperature Oxidation/Corrosion Test failure occurs mostly via two mechanisms: A part may fail due to crack formation, which is primarily induced by thermal fatigue, or the other likely mode of failure results from significant mass loss due to spalling of oxide scale. Resistance to thermal fatigue is determined by a number of material properties, including thermal conductivity, coefficient of thermal expansion, elastic modulus and the cyclic yield strength [3]. Excessive scaling and frequent spalling can lead to rapid loss of a flange's mass and strength. The quenching action which follows each heating cycle is the primary contributor to both thermal fatigue and spalling of the oxide scale. In materials where oxide scale is held loosely against the metallic core, a sudden and relatively large differential contraction between the metallic core and the oxide scale can cause the scale to spall off exposing fresh metal surface. Mass loss will hence continue as the test progresses. In addition, if the density of the oxide scale is significantly lower than that of the metal, then the scale will tend to crack and spall off readily even in the absence of rapid cooling.

Beginning in 1997, when PM stainless steel flanges were first subjected to the HTOT test it was determined that in order for a PM ferritic stainless steel flange to pass the HTOT test, the material should have a minimum sintered density of 7.20 g/cc, and also it should be low in carbon and nitrogen contents. Typically, high temperature hydrogen sintered 409L, 409LE, and 434L materials having this level of sintered density successfully pass the HTOT test. PM materials with lower than 7.20 g/cc density fail due to thermal fatigue [4, 5].

One of the most interesting finding in these tests is that PM stainless steel components (flanges and HEGO bosses) suffer no loss of mass, while wrought stainless steel components exhibit significant loss of mass. In PM stainless steels, the scale once formed, adheres very well to the metallic substrate, whereas the scale formed on wrought stainless steel tends to spall off readily. Wrought stainless steels lose anywhere from 10 to 30% of their mass due to spalling of scale, whereas PM stainless steels gain up to 3% of mass due to adherent scale [4, 6].

The purpose of this investigation was to gain an understanding of the mechanisms behind oxide scale formation and spalling in PM and wrought stainless steels, which produce such differing outcomes. HTOT-tested flanges taken from a recent batch of tests (2005) were utilized in these evaluations. This batch of tests included eight different materials, two of which were wrought stainless steels and one was PM stainless steel. Results of the HTOT test of all eight materials were published at the SAE International Congress 2006 [7].

MATERIALS

All three sets of flanges tested were taken from commercial production lots. All flanges were of two bolt design, measuring approximately 115mm x 65mm. Of the two types of wrought stainless steel flanges one was a flat flange, and the other was a formed flange. The flat flanges (designated as (WFLT) were made from the 410Cb martensitic alloy, and these were heavily oxidized as a result of prior heat treatment. The second type of wrought stainless steel flanges (designated as WFMD) was made from a thin gage sheet (3.5 mm thick) of 409L. The sheet metal was stamped and then cold formed (folded) along the perimeter producing the maximum projection or 'skirt' measuring 25 mm in length. The formed 3-D shape imparted rigidity to the component despite its smaller mass. Also, these flanges derived some of their strength from the cold work imparted during cold forming. The PM stainless steel flanges (designated as PMFLT) were made from 409L powder by compacting to 6.50 g/cc density, followed by sintering at 1288^0C in a 100% hydrogen atmosphere. Chemical compositions of the three types of flanges are shown in Table 1, and their as-received physical characteristics are listed in Table 2.

Table1: Chemical compositions (weight %)

Flange type	Chromium	Carbon	Columbium	Titanium	Silicon	Manganese	Iron
WFLT	11.50	0.12	0.25	0.00	0.25	0.51	Bal.
WFMD	11.13	0.02	0.19	0.30	0.38	0.44	Bal.
PMFLT	11.70	0.02	0.50	0.00	0.80	0.15	Bal.

Table2: Physical characteristics of as-received flanges

Flange type	Density g/cc	Starting stock thickness, mm	Macro hardness HRC/HRB	Microhardness VHN	Overall height mm
WFLT	7.8	9.5	28 HRC	410	9.5
WFMD	7.8	3.5	80 HRB	236	25
PMFLT	7.28	12.5	76 HRB	218	12.5

TESTING

The standard procedure for the High Temperature Oxidation/Corrosion Test (HTOT) is listed in Table 3. Two samples from each type of flanges were included in the test. In a test rack, the samples were suspended vertically from one of the bolt holes, with spacers placed between adjacent samples to help promote uniform heating and quenching.

Table 3: High Temperature Oxidation/Corrosion Test (HTOT)

Each repeat is comprised of four steps as listed below. Typically four repeats are carried out in an eight hour day. A complete test program is comprised off 200 repeats.

Step 1: Soak parts in 5 wt. % sodium chloride solution for 14 minutes.

Step 2: Heat parts in an oven set at 649^0C for 90 minutes, in air.

Step 3: Remove from oven and quickly quench in a bucket of running water, for one minute.

Step 4: Hold samples in a humidity chamber at a temperature of 60^0C and a relative humidity of 85% for at least 20 minutes. Hold samples in the humidity chamber during evenings and weekends.

The test was carried out for 200 repeats, as prescribed. All samples were weighed and photographed at the start of the tests, and thereafter at the completion of the 25th, 50th, 98th, 151st, and 200th repeats. Before each weighing, the flanges were allowed to dry at room temperature over a weekend. Periodically, during the course of the test, the samples were visually examined for onset of any cracking.

At the conclusion of the test, one sample from each pair was sandblasted partially (from mid-length to one end) to permit examination of the metallic surface under the oxide scale. The thickness of the flange stock was also measured before and after sandblasting.

Metallographic examinations were performed on the as-received and the HTOT-tested flange samples. Vickers microhardness measurements were made on samples representing as-received and final-tested conditions. These tests were carried out in a Buehler Model 8540 HT Microhardness Tester using a load of 100 grams.

RESULTS AND DISCUSSION

(a) Physical changes

Table 4 lists mass change data obtained in the test for individual test samples, as well as the average values for each pair of flanges. Both sets of wrought stainless steel samples exhibited increases in mass loss as the test progressed, while the mass of the PM stainless steel samples remained practically unchanged. These samples, in fact, exhibited a very small increase in mass. Spalling of oxide scale was observed to occur during the test in the case of the wrought stainless steel samples. During the first 50 repeats both types of wrought stainless steel flanges showed similar rates of mass loss, and after that the WFMD flanges showed a significantly slower rate of mass loss. In the case of the WFLT flanges, the rate of mass loss remained high throughout the test cycle. In the case of the PM stainless steel flanges (PMFLT), the oxide scale remained firmly attached to the metallic substrate, resulting in a small increase in mass. Figure 1 shows graphically the progression of mass change with test duration.

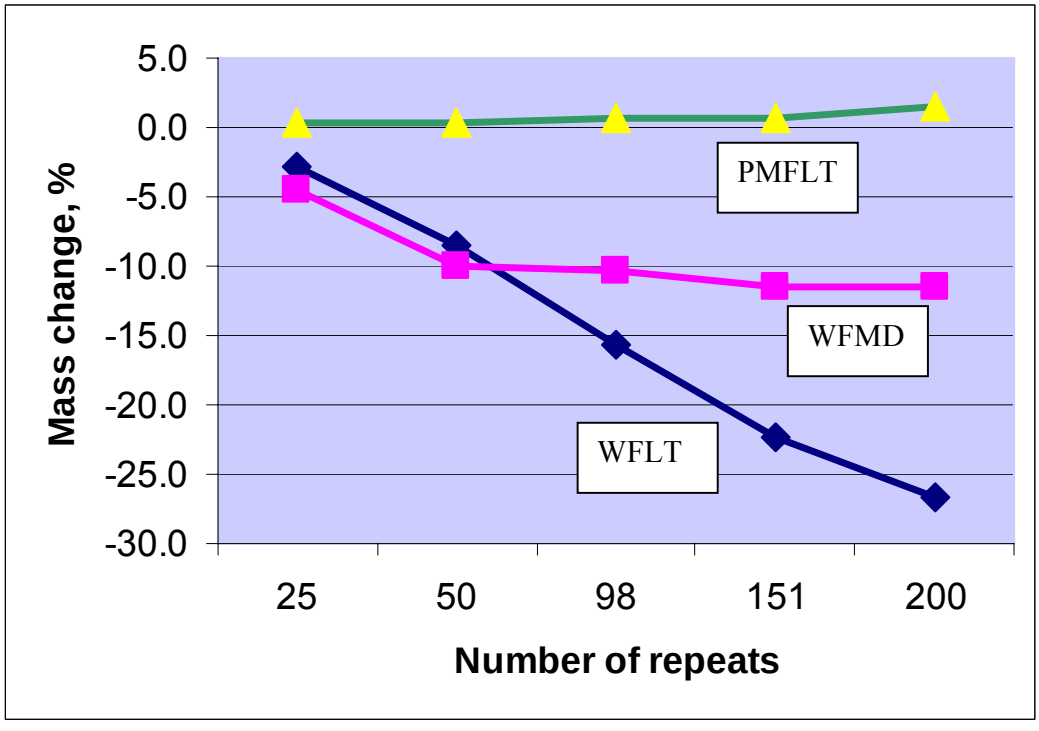

Figure 1: Mass change as a function of test duration

Table 4: Mass change data

Flange type	Sample no.	Original mass, g	Mass change - as % of original mass, at repeats shown				
			25	**50**	**98**	**151**	**200**
WFLT	1	247.7	-2.7	-8.0	-14.1	-20.1	-28.3
WFLT	2	246.7	-3.1	-9.0	-17.1	-24.4	-24.8
Average WFLT			***-2.9***	***-8.5***	***-15.6***	***-22.3***	***-26.6***
WFMD	1	180.0	-5.0	-10.0	-10.5	-12.4	-10.0
WFMD	2	181.3	-4.0	-9.9	-10.1	-10.6	-13.0
Average WFMD			***-4.5***	***-10.0***	***-10.3***	***-11.5***	***-11.5***
PMFLT	1	339.6	0.2	0.4	0.5	0.8	1.0
PMFLT	2	327.3	0.5	0.2	0.9	0.6	1.9
Average PMFLT			***0.4***	***0.3***	***0.7***	***0.7***	***1.5***

Table 5 and Figure 2 show the thicknesses of actual metallic stock remaining at the end of the test, which was determined after removal of oxides scales by sandblasting. PMFLT flanges showed 1% loss in metal stock thickness, while both types of wrought stainless steel flanges lost nearly 30% of their metallic stock thickness due to oxidation and spalling. In the case of WFMD flanges, although the actual loss of thickness was small (1 mm), because of its small starting thickness, the percentage of metal thickness loss was equally high.

Table 5 also shows the changes in microhardness resulting from exposure to the test temperature, for all three materials. The PM 409L material showed a very small decrease in microhardness (by 2.8% from 218 VHN to 212VHN). The wrought 410Cb material underwent an 18% reduction in microhardness, from 410VHN to 336 VHN. This represents a significant loss in the yield strength of the 410Cb martensitic stainless steel resulting from elevated temperature exposure. The wrought ferritic 409L had a higher microhardness in the as-received condition, compared to that of the PM 409L. After undergoing the HTOT test the microhardness of the two materials became almost equal. Hence, it is evident that the difference in microhardness, between the as-received and tested conditions, in the case of the wrought formed 409L material, represents strengthening from the cold work imparted during forming. Figure 3 compares microhardnesses of the three materials in the as-received and tested conditions.

Overall, this study shows that PM 409L stainless steel is only marginally affected by the rigors of the test, while both types of wrought stainless steels undergo significant reductions in mass and microhardness. A reduction in the effective thickness (of metallic stock), combined with a reduction in microhardness can lead to a very significant loss of strength in the case of the flanges made from these two wrought stainless steels.

Table 5: Changes in thickness and microhardness

Flange type	Starting thickness, mm	Thickness after testing, mm		% Loss in metal thickness	Microhardness, VHN		Reduction in microhardness, VHN
		with rust	without rust		Before testing	After testing	
WFLT	9.5	7.1	6.6	30.5	410	336	74
WFMD	3.5	3.2	2.5	28.6	236	213	23
PMFLT	12.5	12.7	12.2	1.0	218	212	6

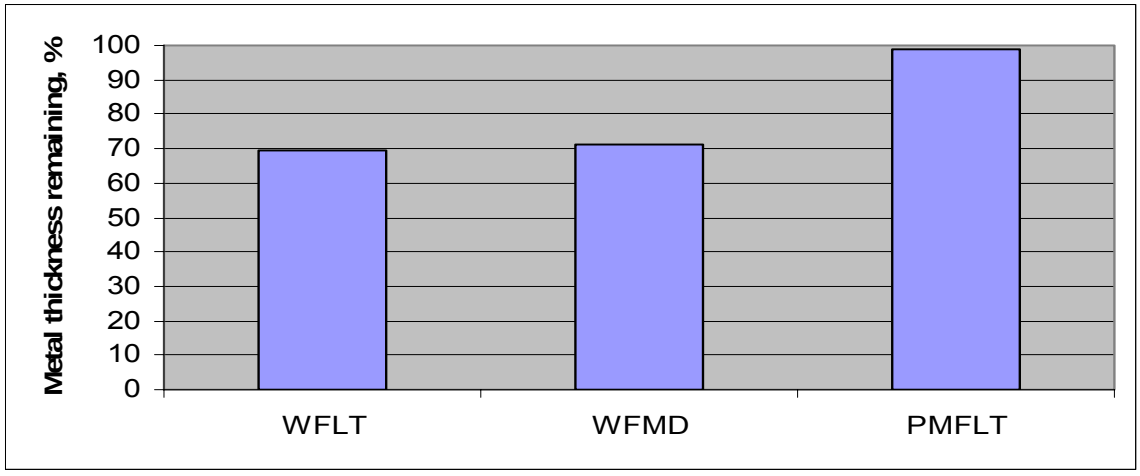

Figure 2: Percentage of original metal stock thickness remaining at the conclusion of the test.

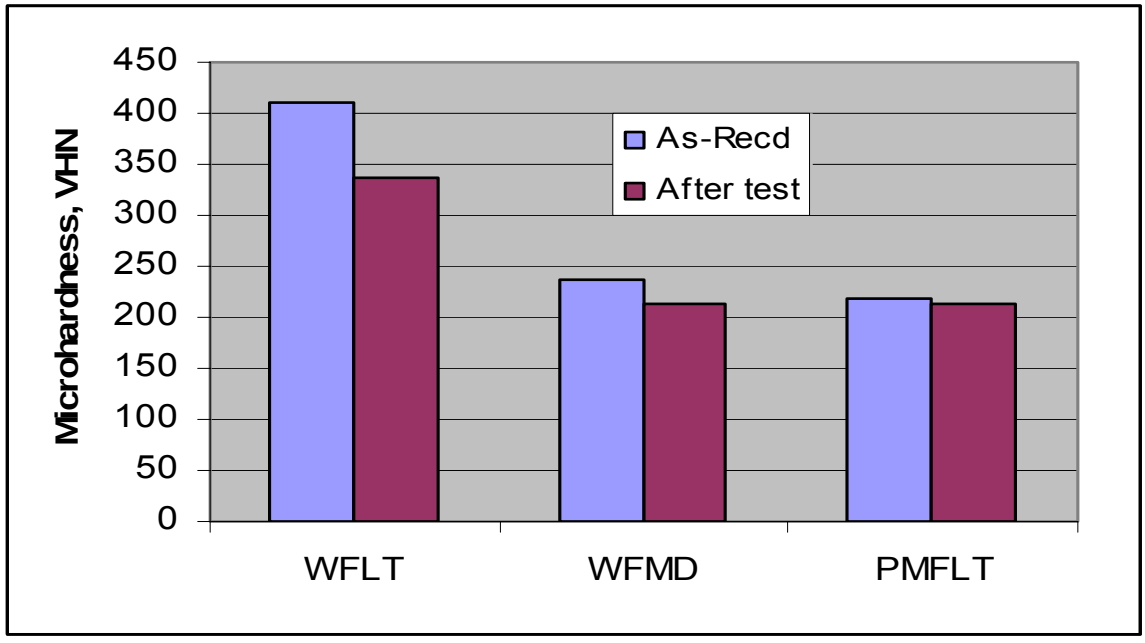

Figure 3: Microhardnesses of samples in the as-received condition and after testing.

(b) Microstructural evaluation of scale

Stainless steels with a chromium content of greater than 14% tend to form protective chromium rich oxides (~ Cr_2O_3), when exposed to elevated temperatures in air. In the case of the lower chromium alloys, such as 409L and 410L, however, the Cr_2O_3 layer is easily penetrated by iron ions leading to the formation of a spinel oxide of the type $FeFe_{2-x}Cr_xO_4$, where $0 < x < 2$, and also formation of iron oxide as an outer layer. Spinel can also form as islands within the iron oxide layer. If the spinel layer cracks, then the underlying chromium depleted metal oxidizes to iron oxide. In either case, a stratified scale is developed on the surface of the part. Depending on the relative diffusion rates of oxygen, and the diffusing metal ions, internal oxidation of the minor element, chromium, can also occur beneath the metal-oxide/metal interface.

In the current study, the three materials, despite being similar in chemical composition, exhibited different spalling behavior. All are low chromium Fe-Cr alloys. Alloy 410Cb has a higher carbon content and is a martensitic alloy. The other two materials have low carbon contents and are ferritic alloys. At the test temperature of 649^0 C one does not anticipate any reaction between carbon and the ambient atmosphere, nor does one expect any nitride formation to occur from reaction with nitrogen in the air. Hence, oxidation is the sole mechanism of degradation in these materials. It is worth noting that the 410Cb is a fine grained material, whereas the other two materials are coarse grained.

Figures 4 and 5 are microstructures of the oxide scale on the WFLT (410Cb) flange at the conclusion of the test. In this material, a clear separation, or crack, is seen at the metal/oxide interface. The scale also consists of cracks running parallel to the interface. The scale is somewhat porous, and it comprises dark and light colored bands. Figure 5 shows a chromium line scan across the oxide scale. The lighter colored layers appear to be oxides of iron only, whereas the darker colored layers are iron and chromium spinels.

Figures 6 and 7 show the microstructures of the oxide scale on the WFMD (wrought 409L) flange at the conclusion of the test. No separation is seen at the metal/oxide interface, although the scale has sustained both longitudinal (parallel to interface) and transverse cracks. The scale here appears to have a higher density compared to what is seen in WFLT. Alternate layers of iron oxide and spinel are present in the scale, as evidenced by the light and dark color bands. Microstructure also shows some penetration of the oxide scale into the metal matrix along grain boundaries. At higher magnification (Figure 7), it is seen that internal oxide networks have formed immediately below the metal surface in the vicinity of grain boundaries. This type of internal oxidation is possible due to the very high activity of chromium coupled with a rapid inward diffusion of oxygen atoms through the oxide scale.

Figures 8 and 9 show the microstructures of the oxide scale on the PMFLT (PM 409L) flange at the conclusion of the test. The scale is free of cracks, and it is much denser compared to the scale on the other two materials. There is no separation, or crack, at the interface of the metal and the scale. At several locations, the oxide scale has penetrated into the metal, aided by surface pores and grain boundaries. This also aided in the formation of sub-surface internal oxidation networks. Figure 8 shows longitudinal (parallel to the interface) propagation of internally oxidized precipitates beneath the metal surface. A line scan taken across the scale confirms that the scale is made up of layers of spinel and iron oxide.

The stronger adhesion of the scale with the metal substrate in the case of the PM material is aided by several factors. Oxide networks and precipitates formed due to internal oxidation have a strong affinity with the oxide scale which leads to formation of strong bonds [8, 9]. This type of phenomenon has been observed by Croll and Wallwork [10]. Internally oxidized particles are also known to act as vacancy sinks and prevent formation of voids at the metal oxide interface [11]. In addition to reducing the possibility of crack formation at the interface, this phenomenon also may have been responsible for the higher density of the oxide scale on the PM material. Surface irregularity of the PM material, stemming from the presence of surface pores, is also considered a contributor to the scale/metal bond.

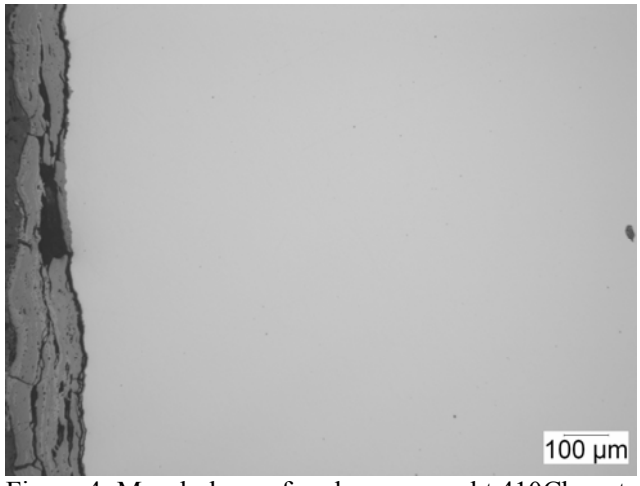

Figure 4: Morphology of scale on wrought 410Cb material (WFLT) showing longitudinal and transverse cracks.

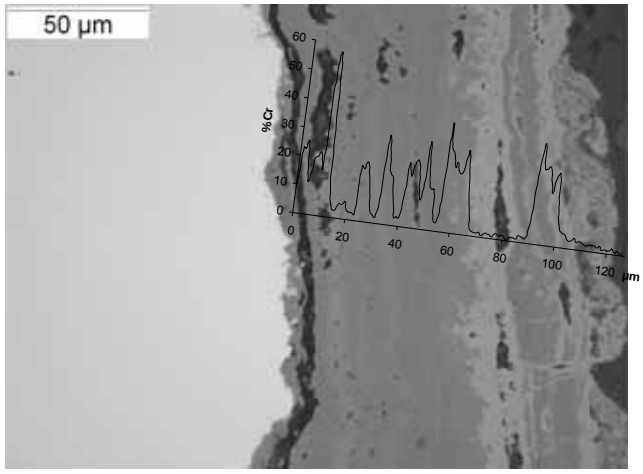

Figure 5: Line scan of scale on wrought 410Cb (WFLT) showing Cr concentration profile.

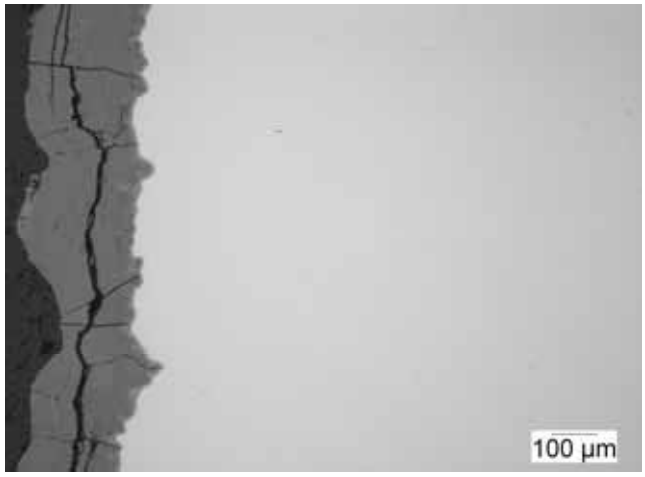

Figure 6: Microstructure of scale on the wrought 409L flange (WFMD) showing longitudinal and transverse cracks.

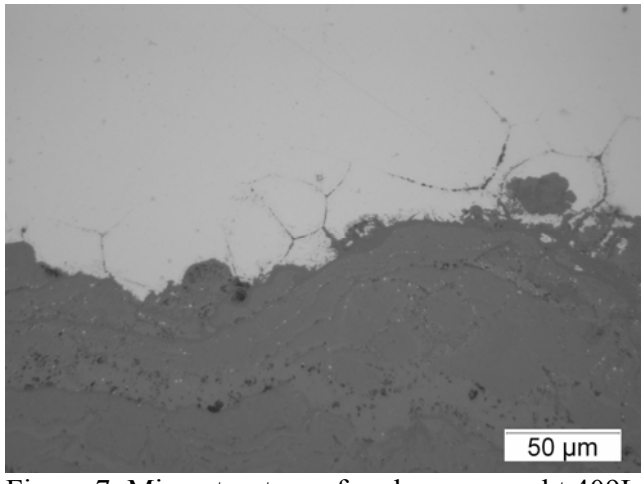

Figure 7: Microstructure of scale on wrought 409L flange (WFMD) showing internal oxide networks in the metal substrate.

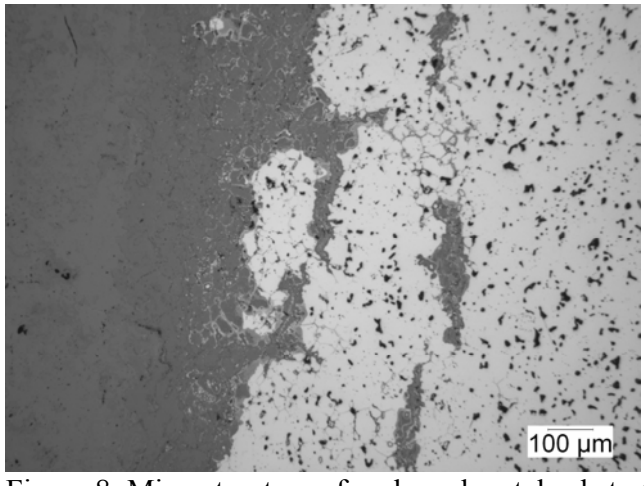

Figure 8: Microstructure of scale and metal substrate in PM stainless steel flange (PMFLT) showing sub-surface internal oxide networks.

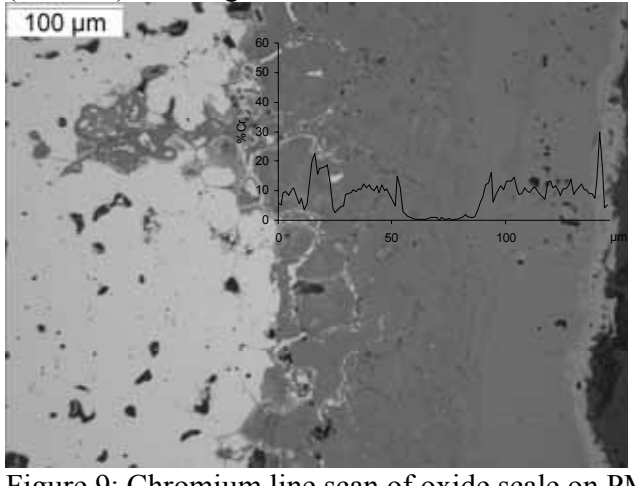

Figure 9: Chromium line scan of oxide scale on PM 409L stainless steel (PMFLT) showing alternate bands of iron oxide and spinel. Anchoring of the scale is also seen at a surface pore.

During thermal cycling, stresses can develop in the oxide scale due to differential expansion and contraction of the metal and the scale. The magnitude of the stress is dependent upon a number of factors, as shown in Equation 1 [8].

$$\text{Stress in the oxide, } \sigma = \frac{E_o \, \Delta T \, (\alpha_o - \alpha_m)}{1 + 2(E_o / E_m)(t_o/t_m)} \qquad (1)$$

Where E_o and E_m are the Young's moduli of the oxide and metal, respectively;
α_o and α_m are coefficients of thermal expansions of the oxide and the metal, respectively;
t_o and t_m are the thicknesses of the oxide and the metal, respectively; and
ΔT is the temperature change.

Stress σ is compressive in nature during cooling (ΔT is positive) , and during heating (ΔT is negative) stress σ is tensile. Hence, greater the difference between the coefficients of thermal expansion of the metal and the oxide, greater is the stress in the oxide scale. The coefficient of thermal expansion of the PM material is lower than that of its wrought counterpart. In this case, the α_m of the wrought 409L and 410Cb is 11.7 x 10^{-6} cm/cm/^{0}C, whereas that for the PM material is 10.9 x 10^{-6} cm/cm/^{0}C. The coefficient of thermal expansion of iron oxide is 9.6 x10^{-6} cm/cm/^{0}C. Based on these values, stress during cooling on the oxide scale of the PM material will be 38% lower than what it is for its wrought counterpart.

During rapid cooling, the scale is unable to contract to the same extent as the metal does, and as a result de-cohesion occurs at the interface. The transverse cracks observed in the oxide layers of the WFMD and WFLT flanges are considered to be the direct result of tensile stresses that develop in the scale during heat up.

According to Equation 1, the ratio of the thickness of oxide to the thickness of the metal ((t_o/t_m) does influence the stress in the oxide. Since, the thickness t_m of WFMD flange is much smaller, compared to that of WFLT (by about 70%), the stress on the scale would be significantly lower for WFMD compared to WFLT. Similarly, the scale on the WFMD flange would have relatively lower stress than the scale on the PMFLT flange, not taking into account the effect of lower coefficient of thermal expansion in the case of PMFLT. In view of this, a wrought ferritic stainless steel flange, having the standard thickness of 9 to 12 mm, would have produced much worse outcome, compared to the WFMD flange.

Although the scale in the WFMD flange developed cracks (both longitudinal and transverse) it did show good bonding with the metal substrate. It is likely that this material underwent an induction period at the start of the test during which internal oxidation along the grain boundaries occurred. Once the internally oxidized precipitates were formed, the scale tended to bond better with the substrate. This may explain why the mass loss was rapid in the beginning of the test, and after about 50 repeats it became much slower. The presence of internally oxidized precipitates also may be responsible for the greater density of the oxide scale, in comparison to that in the WFLT flange.

The oxide scale of WFLT flange exhibited all of the undesirable characteristics previously discussed. There was a greater incidence of separation between the scale and the metal. The oxide scale was of lower density and had multiple longitudinal and transverse cracks. In this material no internal oxidation networks or precipitates were present. It is likely that due to the fine grained structure of the metal, outward diffusion of chromium was too fast to permit any formation of internal oxide precipitates. Absence of internally oxidized precipitates has possibly led to poor

bonding of the scale to the metal substrate. There were fewer transverse cracks in the WFLT flange as compared to the WFMD flange. This may be due to the presence of multiple longitudinal cracks leading to greater incidence of separation between the scale and the metal substrate.

To summarize, the superior bonding of scale to the metal surface in the case of the PM stainless steel is primarily promoted by the presence of sub-surface internal oxides, as well as the smaller difference between the coefficients of thermal expansion of the PM stainless steel and the scale. The inherent surface porosity of the PM stainless steel is considered a secondary contributor to scale/metal bonding. The wrought formed stainless steel flange also benefited from sub-surface internal oxidation after an initial induction period, which led to a reduced rate of spalling after 50 repeats. The relatively thinner metal stock thickness of these flanges is considered to have resulted in lower stress levels in the scale, compared to what would be expected in the standard thickness flanges of similar material. Despite this, longitudinal and transverse cracks were formed in the scale of this material. The 410Cb martensitic stainless steel, owing to its finer grain structure, did not develop internal oxides, and as a result did not develop strong scale/internal oxide bonds. This, combined with the higher levels of stress developed in the scale (per Equation 1), led to de-cohesion at the interface and development of both longitudinal and transverse cracks in the oxide scale.

CONCLUSIONS

- Exhaust flanges made of PM ferritic stainless steel 409L show significantly better performance over the wrought stamped 410Cb flanges and the wrought formed 409L flanges in High Temperature Oxidation/corrosion Test. Both of these wrought stainless steels suffer as much as 30% loss in metal mass due to spalling, whereas the PM stainless steel retains nearly 99% of its original mass. Both wrought stainless steels also suffer significant reductions in microhardness, whereas the PM stainless steel undergoes a minimal change in microhardness.
- Poor bonding of the oxide scale on to the metal substrate is responsible for the high rate of spalling in the two wrought stainless steels evaluated.
- Good adherence of the oxide scale on the PM stainless steel flanges results from the scale/internal oxide bonding, as well as from the anchoring of the scale in the surface pores.
- The lower coefficient of thermal expansion of the PM stainless steel leads to a reduction of thermal stresses in the scale during thermal cycling, which also contributes to avoidance of spalling.

REFERENCES

1. Armco Steel Product Data Sheet, No. S-32, “Armco 410 Cb Stainless Steel”, Published by Armco Steel Co, Middletown, Ohio.

2. G. L. Ramsey G.E. Regan P. A. dePoutiloff, and P. K. Samal, “P/M Stainless Steel Flanges and Sensor Bosses Meet Critical Qualification Requirements for Exhaust Applications”, presented at SAE International Congress and Exposition, March, 2000, SAE Paper No2001-01-1002.

3. George Dieter, Mechanical Metallurgy, McGraw Hill Publications, New York, First Edition, 1961, pp 333 -334.

4. S. O. Shah, J. R. McMillen, P. K. Samal, and E. Klar, “Development of Powder Metal Stainless Steel Materials for Exhaust System Applications“, presented at SAE International Congress and Exposition, February 1998. Paper No. 980134.

5. T. Hubbard, K. Couchman, and C. Lall, “Performance of Stainless Steel P/M Materials in Elevated Temperature Applications”, presented at SAE International Congress and Exposition, February 1998, SAE Paper No: 980326.

6. T. Hubbard, K. Couchman, and C. Lall, “Performance of Stainless Steel P/M Materials in Elevated Temperature Applications”, presented at SAE International Congress and Exposition, February, 1997, SAE Paper No: 970422.

7. S. Thakur, J. R. McMillen, M. L. Holly, and P. K. Samal, “High Temperature Oxidation/Corrosion Performance of Various Materials for Exhaust System Applications”, presented at SAE International Congress and Exposition, April 2006, SAE Paper No: 2006-01-0605.

8. A. S. Khanna, “Introduction to High Temperature Oxidation and Corrosion”, ASM International, Materials Park, Ohio, 2002, p 212.

9. L. A. Morris, ‘Resistance to Corrosion in Gaseous Atmospheres”, in Handbook of Stainless Steels, D. Peckner and I. M. Bernstein, editors, McGraw-Hill Book Company, New York, 1977., pp 17-1 to 17-28.

10. J. E. Croll and G. R. Wallwork, “Oxidation of Metals”, vol. 1, p. 55, 1969.

11. J. M. Francis and J. A. Jutson, in Corrosion Science, vol. 8, 1968, p. 445.